Dynamic Solvation of Aminophthalimides in Solvent Mixtures

Diana E. Wetzler,[†] Carlos Chesta,[‡] Roberto Fernández-Prini,[†,§] and Pedro F. Aramendía*[,†]

INQUIMAE and Departamento de Química Inorgánica, Analítica y Química Física, FCEN, Universidad de Buenos Aires, Pabellón 2, Ciudad Universitaria, C1428EHA Buenos Aires, Argentina, Departamento de Química y Física, Universidad Nacional de Río Cuarto, 5800 Río Cuarto, Argentina, and Unidad de Actividad Química, CNEA, Libertador 8250, 1428 Buenos Aires, Argentina

Received: May 14, 2001; In Final Form: November 30, 2001

The solvatochromism and thermochromism of 4-aminophthalimide and 4-amino-*N*-methylphthalimide were studied by absorption and steady state and time-resolved fluorescence emission in solvent mixtures of toluene−ethanol and toluene−acetonitrile in the temperature range 5−70 °C. The wavelengths of the maximum of absorption and of fluorescence emission shift to the red with the increase of the proportion of the polar component in the mixture. The greater affinity for the polar component of the mixture of the excited state compared to the ground state enhances preferential solvation, which is the origin of this red shift. On the other hand, a spectral shift to the blue is found upon temperature increase in solvent mixtures. This fact can be explained by considering that association of the polar component with the excited-state solute is exothermic and decreases with temperature. The appointed solvation change is attained by diffusion-controlled exchange of solvent molecules between the bulk and the solvation sphere. This process leads to a time-dependent emission spectrum in the nanosecond time domain. In this work a kinetic scheme is developed to describe this exchange and explain the time-dependent fluorescence emission spectra. The description is based on a Langmuir type association of the solvent molecules with the solute. The solvation equilibrium is attained by stepwise solvent exchange. The kinetic data and the spectral information are integrated in a thermodynamic cycle that can describe the solvation of excited and ground states at any solvent composition.

Introduction

Solvation involves all the interactions of a solute with the solvent. These interactions can be rather arbitrarily grouped in nonspecific and specific ones.[1] The former are dependent on electrostatic characteristics of solute and solvent such as charge, dipole and quadrupole moments, and dielectric constant, as well as polarizabilities. These interactions if homogeneous can be modeled at a continuum or microscopic level.[2−4] On the other hand, the so-called specific interactions depend on the chemical nature of solute and solvent and include hydrogen bonding and repulsive interactions such as "size" (taken into account in the form of a suitable molecular radius) and "shape" (excluded volume). The difficulty of considering all the effects responsible for solvation in an analytical treatment is bypassed by the introduction of the empirical parameters of solvation.[1,5] Many of these parameters are based on the solvatochromism of different medium-sensitive solutes also called solvation probes. The origin of solvatochromism, which can be measured in absorption or in emission, is the different equilibrium solvation of the ground and the excited states of the solute.

Solvation in solvent mixtures has an additional effect originated on the different interaction energy of the solute with the solvent mixture components.[1,6] This fact can cause the solvation sphere composition to differ from the mean composition of the solvent. Suppan[7,8] took this effect into account by a continuum dielectric approach and introduced the concept of dielectric enrichment to describe the concentration enhancement of the more polar component of the solvent mixture in the vicinity of a polar solute.

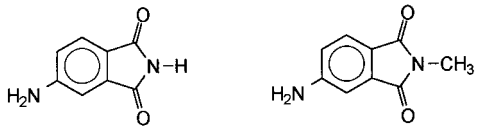

Figure 1. Structures of 4-aminophthalimide (AP) and 4-amino-*N*-methylphthalimide (AMP).

Light absorption by a solute induces a very fast change in electron density, which displaces the solute and its surroundings from equilibrium with respect to the nuclear coordinates. The system attains equilibrium by nuclear relaxation of the probe and solvation sphere. This takes a few picoseconds in common fluids near room temperature.[9,10] In solvent mixtures, instead of only rotation as in the case of pure solvents, an eventual change in the composition of the solvation sphere after excitation to attain equilibrium with the excited state must take place by diffusion-controlled exchange of solvent molecules with the bulk.[7,8,11] The rate of this process depends on temperature and solvent composition and can lead to a time-dependent emission spectrum or dynamic solvatochromism.

Aminophthalimides have been extensively used as strong fluorescent probes.[12−21] This is the case of 4-aminophthalimide (AP) and its derivative 4-amino-*N*-methylphthalimide (AMP) (Figure 1), which exhibit the common emission feature of

* Correspondence author. E-mail: pedro@q1.fcen.uba.ar. Fax: 54 11 4576 3341.
[†] Universidad de Buenos Aires.
[‡] Universidad Nacional de Río Cuarto.
[§] CNEA.

10.1021/jp0118423 CCC: $22.00
Published on Web 02/26/2002

compounds with an electron-donating moiety (the amino group) and an electron acceptor moiety (the carbonyl of the imido group) placed in the *para* position in a benzene ring. The Stokes shift of this internal charge transfer (ICT) emission is very sensitive to the polarity and hydrogen bond donating (HBD) ability of the medium. The ICT character of the transition causes a dipole moment increase upon excitation from 3.5 to 6.5 D.[7] A time-dependent fluorescence spectrum was informed in neat solvents at low temperature.[10,13−15] This effect was attributed to solvent reorientation. Time-dependent fluorescence spectra were also observed in solvent mixtures at higher temperature.[13,21]

The different behavior of the fluorescence of AP in protic and aprotic solvents was attributed to a solvent-mediated tautomerization[14] or proton transfer.[18] Evidence for this comes from NMR studies, the deuterium isotope effect in the fluorescence, and ab initio calculations. Comparing the behavior of fluorescence in neat water and in D_2O, the authors conclude that emission originates in the proton-transferred species formed in less than 1 ps in the excited state. A tautomerization involving a cyclic AP−solvent complex is postulated. In this work, we compare the behavior of AP and AMP to estimate the viability of this hypothesis.

In neat solvents, Rapp et al.[22] developed a kinetic scheme to describe the time-dependent spectral shift by stepwise reorientation of solvent molecules in the solvation sphere. This model leads to the Bakhshiev's formula[9,23] for the dependence of the mean energy of the emission with time, which is monoexponential. The spectral shift of AP is monoexponential in tetrahydrofuran[14] and biexponential in alcohols.[10,14]

Due to their big solvent-dependent spectral shifts, AP and AMP are ideal for monitoring solvation changes, especially in a mixture of a polar and a nonpolar component. In this work, we present absorption, steady state, and time-resolved spectroscopic studies of AP and AMP in mixtures of ethanol−toluene and acetonitrile−toluene as a function of composition and temperature. The solvatochromism, thermochromism, and emission decay kinetics are explained on the basis of a remarkable difference in solvation between ground and excited states. We further develop a kinetic scheme to obtain characteristic times for solvent exchange in the ground and excited states. Finally, we integrate spectral and kinetic data in a thermodynamic cycle that describes the different solvation of the ground and excited states of AP in the mixtures.

Experimental Section

Chemicals. AP (Acros Organics) of 97% purity was recrystallyzed from ethanol. AMP (Aldrich) was used as received. Solvents toluene (tol) (Merck, Uvasol), acetonitrile (acn) (Merck, pa), trifluoroethanol, triethylamine, and ethanol (95% v/v) (eth) (Merck, for spectroscopy) were used as received.

Solvent Mixtures. They were prepared by mixing known volumes of each solvent. In this way, the mole fraction of solvent is known in the mixture. To obtain the molar concentration of the minor component, literature values for the mixture density at 25 °C were used.[24] The temperature effect on concentration was neglected.

Absorption and Emission Spectra. Absorption spectra were recorded on a Shimadzu PC-3100 spectrophotometer. Corrected fluorescence emission and excitation spectra were recorded under steady-state conditions in a PTI-Quantamaster apparatus. Time-resolved fluorescence decays were measured on time-correlated single photon counting equipment (Edinburgh Series 9000). Time-resolved spectra were reconstructed from decay curves registered at different emission wavelengths under all other identical conditions. In all cases, temperature was controlled by external water circulation and measured in the cuvette with a calibrated thermistor. The fit of the kinetic data was performed by global analysis of the decay traces at different wavelengths.

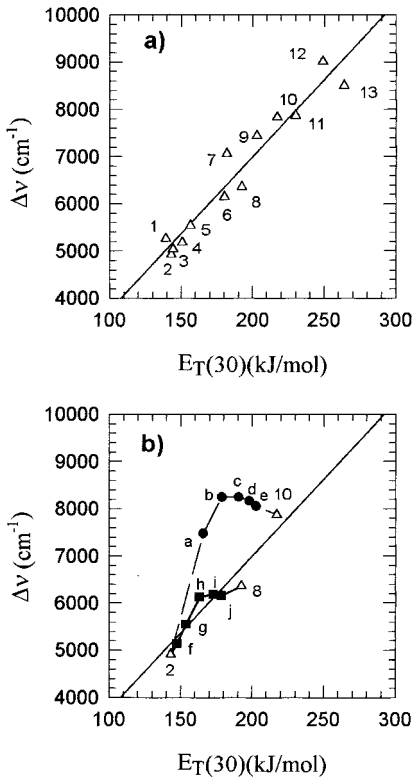

Figure 2. Stokes shift for AP as a function of $E_T(30)$ at 27 °C. (a) Triangles represent the values for neat solvents: 1, triethylamine; 2, toluene; 3, diethyl ether; 4, dioxane; 5, tetrahydrofuran; 6, acetone; 7, *tert*-butanol; 8, acetonitrile; 9, 2-propanol; 10, ethanol; 11, methanol; 12, trifluoroethanol; 13, water (solvents 3−7, 9, 11, and 13 from refs 16 and 32). (b) Points 2, 8, and 10 values in pure solvents as in (a). Dark circles represent the values in toluene−ethanol mixtures at [ethanol]/*M* of the following: a, 0.145; b, 0.429; c, 1.36; d, 4.40; e, 7.04. Dark squares represent the values in toluene−acetonitrile at [acetonitrile]/*M* of the following: f, 0.157; g, 0.613; h, 1.46; i, 4.75; j, 7.60. In both plots the line is the best linear fit for neat solvents.

Semiempirical Calculations. These were performed under the AM1 approximation with the AMPAC program (version 6.55, Semichem, Inc., Shawnee, KS). The ground-state and the excited-state equilibrium geometries were achieved by performing a configuration interaction calculation (CI) with 396 microstates. These many states were obtained by single and double excitation, using CI = 24.

Results

Solvatochromism. Absorption and emission spectra in pure solvents shift to the red upon solvent polarity increase. The Stokes shift ($\Delta\nu$) displays a linear correlation with the $E_T(30)$ parameter in neat solvents that can be described by the equation $\Delta\nu$ (cm^{-1}) = 32.55$E_T(30)$ (kJ/mol) + 492, as shown in Figure 2. A representation of $\Delta\nu$ as a function of the HBD parameter α gives a linear representation of similar quality with a correlation $\Delta\nu$ (cm^{-1}) = 1989.5α + 6004.5 for the solvents with $\alpha \neq 0$.

Figure 2 also shows the Stokes shift in tol−eth and in tol−acn mixtures. The Stokes shift in tol−eth mixtures can be clearly distinguished from the neat solvents of similar $E_T(30)$. This indicates that the polar solvent enrichment by aminophthalimides

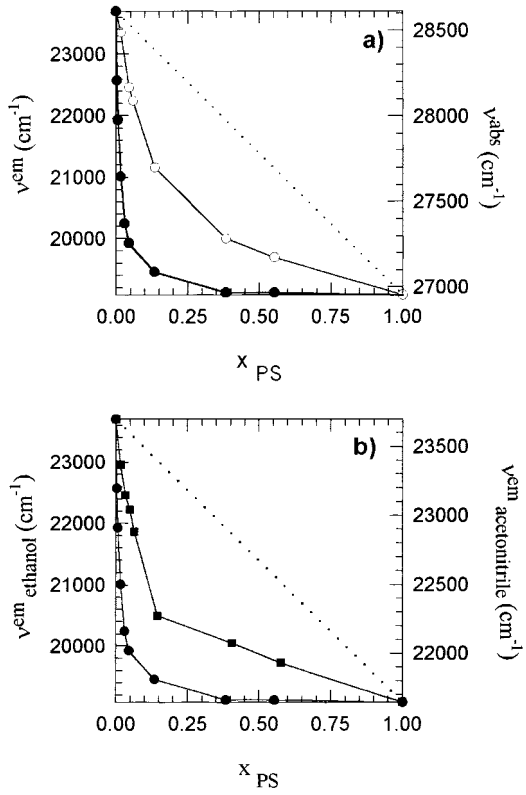

Figure 3. (a) Wavenumber of the maximum of the fluorescence emission spectrum (dark circles) and of the absorption spectrum (open circles) of AP in toluene−ethanol as a function of the molar fraction of ethanol. (b) Wavenumber of the maximum of the fluorescence emission spectrum of AP as a function of the molar fraction of the polar solvent in toluene−ethanol mixtures (dark circles) and in toluene−acetonitrile mixtures (dark squares).

in these mixtures is different from the enrichment of the probe $E_T(30)$. Additionally, we cannot discard the possibility that the emission of aminophthalimides originates in nonequilibrated excited states. We present evidence of this fact below, which certainly contributes appreciably to the different behavior of AP and AMP in the mixtures compared to neat solvents.

Figure 3 shows the energy of the absorption and emission maxima as a function of solvent composition in tol−eth mixtures and the emission maxima in tol−acn. The spectral shift is greater in tol−eth mixtures than in tol−acn mixtures, in accordance with the greater difference between the maxima of absorption and emission in the neat solvents of each mixture (see Figure 2). At [eth] = 0.145 M, which corresponds to a mole fraction of ca. 1%, the emission energy is midway between the values of the neat solvents. This indicates a strong preferential solvation by ethanol as it was already reported by Suppan[7,8] for other solvent mixtures. A similar result was reported in mixtures of 2-propanol−supercritical CO_2 for AMP[21] and in mixtures of 2-propanol−toluene for AP.[13] In tol−acn mixtures, a 1% mole fraction of acn shifts the emission maximum to the red by 25% of the difference between tol and acn. This indicates that the difference in affinity between the ground state and the excited state of aminophthalimides is greater for eth than for acn. The bathochromism in absorption is less pronounced.

Thermochromism. Absorption and emission spectra shift to the blue upon temperature increase in all cases. The magnitude of this shift is much greater for emission than for absorption, and it is also greater in solvent mixtures than in neat solvents. Figure 4 shows the energy of the emission maximum of the corrected steady-state spectra of AP in tol−eth. Similar results

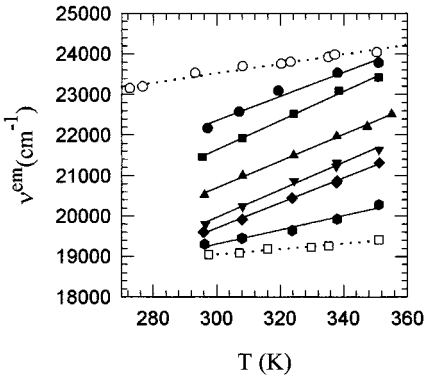

Figure 4. Wavenumber of the maximum of the fluorescence emission spectrum of AP in toluene−ethanol mixtures as a function of temperature. The curves, from top to bottom, correspond to the following solvent compositions: pure toluene; [ethanol]/M = 0.029, 0.059, 0.145, 0.289, 0.429, and 1.36; pure ethanol.

TABLE 1: Temperature Coefficient for the Variation of the Energy of the Emission Maxima of AP in Toluene−Ethanol and in Toluene−Acetonitrile

toluene−ethanol		toluene−acetonitrile	
solvent composn	slope (J•mol^{-1}•K^{-1})	solvent composn	slope (J•mol^{-1}•K^{-1})
toluene	137	toluene	137
[ethanol] = 0.030 M	355		
[ethanol] = 0.060 M	429		
[ethanol] = 0.145 M	394	[acn] = 0.157 M	162
[ethanol] = 0.29 M	408	[acn] = 0.31 M	177
[ethanol] = 0.43 M	369		
[ethanol] = 1.35 M	206	[acn] = 1.46 M	190
ethanol	80	acetonitrile	87

are obtained for AMP. The magnitude of the thermochromic shift is much smaller in tol−acn mixtures, thus paralleling the smaller solvatochromic shift in these mixtures.

The temperature coefficients of the plots of Figure 4 are summarized in Table 1, which includes results for tol−eth and tol−acn mixtures. To obtain the values of Table 1, a linear dependence was assumed between the energy of the emission maximum and temperature at each solvent composition.[25] This temperature coefficient has units of entropy and, according to eq 1, can be interpreted as a positive entropy change upon emission.

$$-h\nu_{max}^{em} = A + BT = \Delta H_{e\rightarrow g} - T\Delta S_{e\rightarrow g} \qquad (1)$$

The absolute magnitude of the temperature coefficient has a maximum at [eth] ≈ 0.1 M. The values for the mixtures are systematically bigger than the values for the pure solvents. If the observed linear dependence of the emission maxima with temperature is extended to a broader temperature range, inconsistencies arise in the predicted value of emission maxima. This point is discussed later (see Discussion).

Semiempirical Calculations. The spectral behaviors of AP and AMP are similar. Though the imido hydrogen, which is only present in AP, is a potential interaction site with the medium, this interaction does not play a role in the fluorescence behavior. To exclude any effect that the imido hydrogen might have in the interaction with the solvent that is not seen in the spectral features, only calculations for AMP were carried out.

Figure 5 shows the Mulliken charges in the equilibrated ground state and in other three states: the Franck−Condon state after light absorption; the relaxed excited state; the Franck−Condon state after emission.

Light absorption is accompanied by a negative charge shift from the amino nitrogen to the aromatic ring. In the relaxed

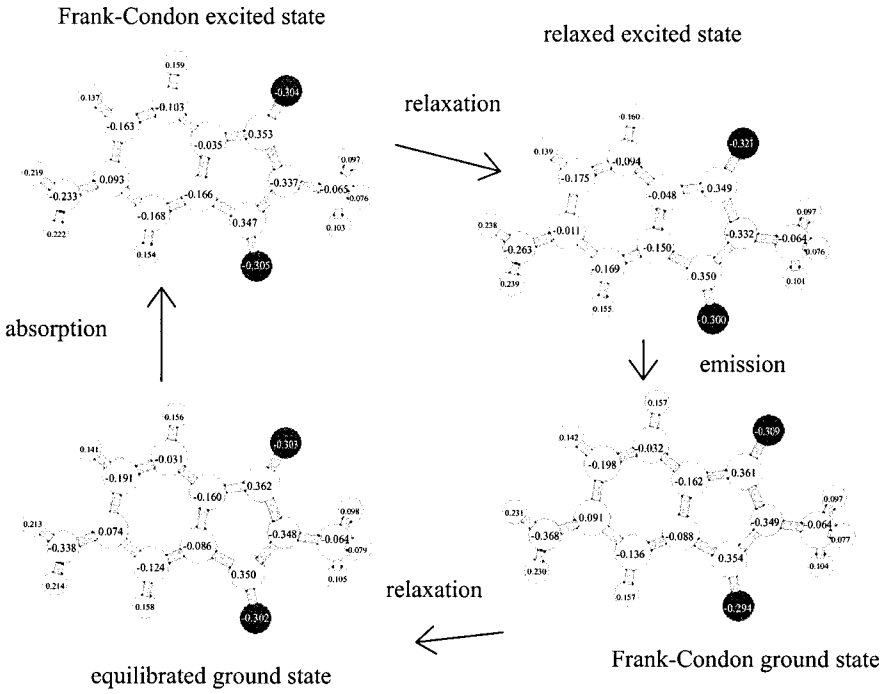

Figure 5. Mulliken charges for AMP in the equilibrated ground state, in the Franck−Condon state after light absorption, in the relaxed excited state, and in the Franck−Condon state after emission.

excited state, the amino group becomes coplanar to the aromatic ring. The relaxation in the excited-state surface localizes the negative charge on the oxygen of the carbonyl in the *para* position to the amino group, as found for similar donor−acceptor compounds.[14,26]

The association of ethanol molecules with ground-state AMP takes place as a consequence of hydrogen bond formation, which is possible in three different positions: the two carbonyl groups and the amino group. The interaction energy in these three sites is negative and very similar: -19 ± 1 kJ/mol.[27] In the excited state, the interaction energy is slightly greater in magnitude, involving -24 ± 1 kJ/mol in any of the same three locations.

In the interaction with the carbonyl groups, ethanol acts as HBD. In the ground state, the association enhances the negative charge of the oxygen atom where ethanol is bonded. Nevertheless in the relaxed excited state the negative charge increase locates always at the oxygen atom of the carbonyl in the *para* position to the amino group. The interaction energy of AMP associated with two ethanol molecules in any two of these sites is additive. In the interaction with the amino group, AMP acts as the HBD.

Calculations predict that acetonitrile binds preferentially by hydrogen bond formation with the amino group. The calculated interaction energy is -6 and -10 ± 1 kJ/mol, with the ground and excited states, respectively.

Kinetics of Fluorescence Decay. In neat solvents, emission spectra are time independent near room temperature in the nanosecond time range. The spectral shift observed for AP or AMP in other works either takes place at lower temperatures in the nanosecond time range or is faster at room temperature.[10,13−15] This effect is due to solvent reorientation.

On the other hand, emission spectra shift to the red as a function of time in all solvent mixtures studied. This is depicted in Figure 6 for selected cases. Our observation is in agreement with a report of time-resolved fluorescence emission of AMP in mixtures of 2-propanol in supercritical CO_2.[21] Furthermore, this is also to be expected for probes such as AP and AMP with a great difference in solvation in the ground and excited states, as discussed by Suppan.[7,8]

The evolution of the emission spectra can be roughly described as a fast red shift of the spectrum followed by a slower decay of the total emission with an essentially fixed spectrum. The kinetics of the red shift is faster at higher temperature and at higher concentration of the polar solvent. AP and AMP behave in the same way, ruling out an excited-state tautomerization involving the imido hydrogen as being responsible for these features of fluorescence decay in solvent mixtures, even when they contain a protic component.[14,18] The shift of the spectrum takes place with a characteristic lifetime between 2 and 7 ns (depending on the temperature) in [eth] = 0.145 M in toluene. The total fluorescence decay takes place with a characteristic lifetime of ca. 15 ns, which is temperature independent and very similar to the decay lifetime of aminophthalimides in aprotic neat solvents[16] and in 2-propanol.[10,13]

The fast process can be assigned to diffusion-controlled solvent exchange, whereas the solvation equilibrated decay of the total excited-state population is responsible for the slower process observed.

Due to the limited amount of traces recorded at different wavelengths, to pick out the energy of the maximum of the emission requires fitting the spectra to a suitable function. The continuous lines of Figures 6 and 7 represent the fit of the data to a Gaussian distribution of emission intensity as a function of wavenumber, as described by

$$I(\nu,t) = I_{max}(t)\exp\left[-\frac{(\nu - \nu_{max}(t))^2}{2.\sigma(t)^2}\right] \qquad (2)$$

In eq 2, the fitting parameters are $\nu_{max}(t)$, the time-dependent wavenumber of the maximum of the spectrum, $I_{max}(t)$, the intensity at the maximum, and $\sigma(t)$, the width of the distribution. The fits and the spectra coincide within 2%, so the quality of

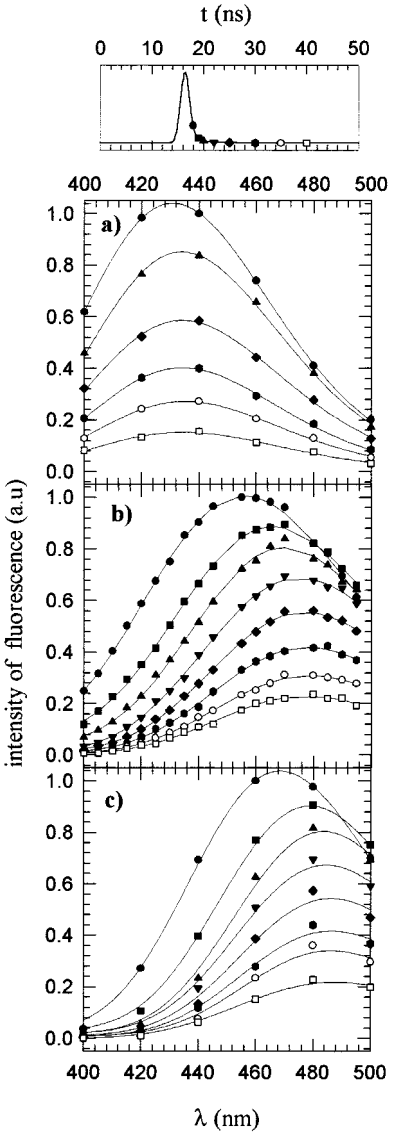

Figure 6. Time-resolved emission spectra in solvents mixtures, at 27 °C. Top scheme: time profile of the excitation pulse. Key: (a) AP in toluene−acetonitrile, [acetonitrile] = 0.157 M; (b) AP in toluene−ethanol, [ethanol] = 0.145 M; (c) AMP in toluene−ethanol, [ethanol] = 0.145 M. The time at which each spectrum was taken is indicated by the corresponding symbol in the pulse profile. Continuous lines represent the fit of the data to a Gaussian distribution.

the fits is considered satisfactory. The parameter $\sigma(t)$ decreases with time from a value of ca. 1800 cm^{-1} to a value of ca. 1600 cm^{-1}, which in all cases is completed during the excitation pulse and which is temperature independent. We attribute this decrease to the extinction of a contribution of spurious light from the excitation pulse. Figure 8 shows the dependence of $I_{max}(t)$ and $\nu_{max}(t)$ with time. Their behavior can be well represented by monoexponential decays, where the lifetime for $\nu_{max}(t)$ is smaller than the lifetime for $I_{max}(t)$. The rate constants obtained according to this analysis are summarized in Table 2, where they are compared to rate constants obtained with the kinetic analysis developed later in this work.

The extent of the red shift decreases with temperature. The difference in emission maximum between the first discernible spectrum and the emission spectrum at $t > 30$ ns, when spectral shift is complete, is 1900 cm^{-1} at 6 °C and 1200 cm^{-1} at 61 °C for [eth] = 0.145 M in toluene.

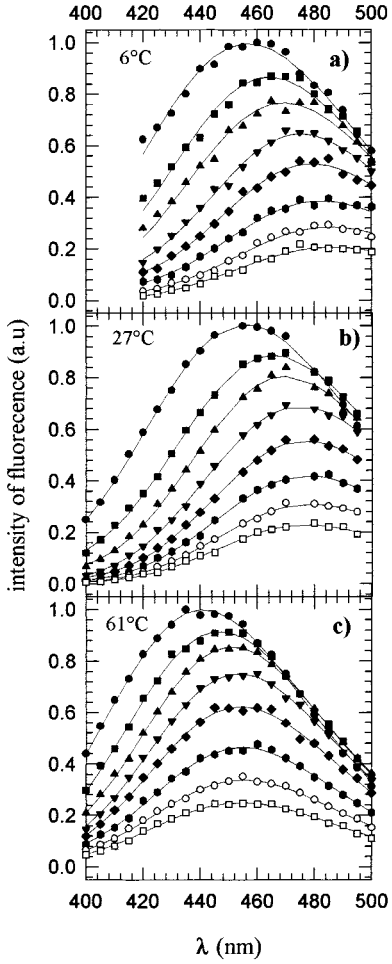

Figure 7. Time-resolved emission spectra for AP in toluene−ethanol mixtures, [ethanol] = 0.145 M, at different temperatures: (a) 6 °C; (b) 27 °C; (c) 61 °C. Continuous lines represent the fit of the data to a Gaussian distribution. Time profile of the excitation pulse and time of each spectrum are as in Figure 6.

The decay kinetics of the fluorescence, monitored at a fixed wavelength, is not single exponential. As discussed above, at least two lifetimes are needed to describe the kinetics. The most elemental kinetic scheme to explain this behavior is described by eqs 3 and coincides with the one proposed by Betts and Bright:[21]

$$\mathrm{AP}^* \xrightarrow{k_0} \mathrm{AP}$$

$$\mathrm{AP}^* + \mathrm{PS} \xrightarrow{k_d[PS]} (\mathrm{AP{-}PS})^*$$

$$(\mathrm{AP{-}PS})^* \xrightarrow{k_{-d}} \mathrm{AP}^* + \mathrm{PS}$$

$$(\mathrm{AP{-}PS})^* \xrightarrow{k_0} \mathrm{AP{-}PS} \qquad (3)$$

In eq 3, PS represents a polar solvent molecule. AP is a solute molecule with a ground-state equilibrated solvation sphere. AP−PS represents a solute molecule that has an additional PS molecule associated, compared to AP. We assume that AP* and (AP−PS)* decay with the same probability. This assumption is supported by the fact that the longer decay time is independent of solvent composition in the range of interest for the kinetic measurements ([PS] < 1.5 M).

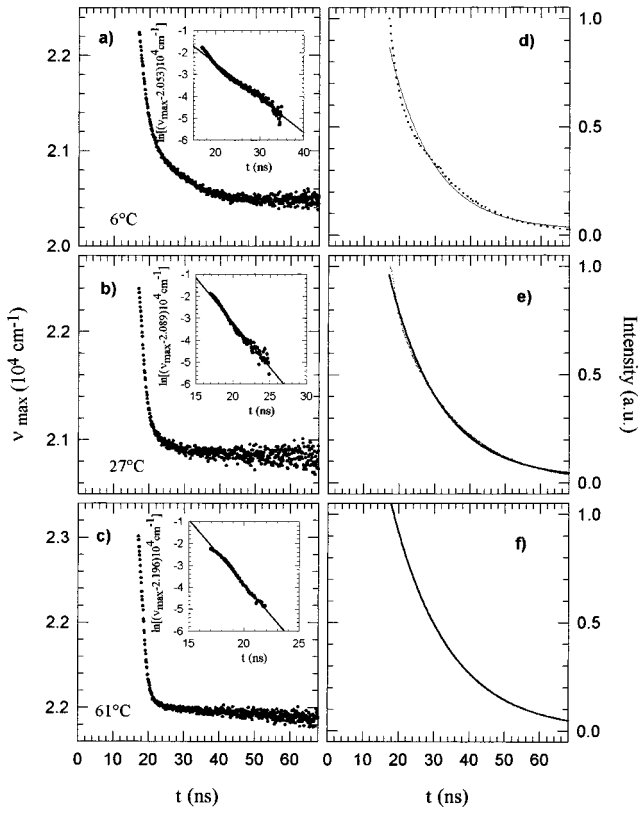

Figure 8. Time dependence of spectral parameters for AP in toluene−ethanol, [ethanol] = 0.145 M [(a)−(c)], wavenumber of the maximum of the emission spectrum [insets represent first-order decay of ν_{max}, [(d)−(f)], and intensity at the maximum. Plots correspond to different temperatures: (a, d) 6 °C; (b, e) 27 °C; (c, f) 61 °C.

TABLE 2: Rate Constants for Spectral Shift and Total Fluorescence Decay, Compared to the Corresponding Values Obtained from the Solvent Exchange Dynamics[a]

	spectral shift and decay		solvent exchange kinetics	
T (°C)	k_{ex} (ns^{-1})[b]	k_0 (ns^{-1})[c]	k_{ex} (ns^{-1})	k_0 (ns^{-1})
6	0.158	0.081	0.179	0.093
27	0.408	0.069	0.427	0.066
61	0.587	0.062	0.700	0.066

[a] Values for AP in toluene−ethanol mixtures, [eth] = 0.145 M. [b] First-order rate constant for the decay of the spectral shift [c] First-order rate constant for the decay of the fluorescence intensity at the time-dependent maximum of emission.

Such a mechanism has two relaxation times (τ_1 and τ_2), given by

$$1/\tau_1 = k_0$$

$$1/\tau_2 = k_0 + k_{-d} + k_d[\mathrm{PS}] \qquad (4)$$

The emission decays were fitted to a sum of two exponentials to obtain τ_1 and τ_2. According to the previous considerations, $\tau_2 < \tau_1$. For the decays of AP in neat solvents, acn, tol, and eth, as well as for the decay of AP in tol−eth, [eth] = 0.145 M, and in tol−acn, [acn] = 0.157 M, and for the decay of AMP in tol−eth, [eth] = 0.145 M, a global analysis of the traces obtained at fixed wavelengths was performed. In the remaining media, a biexponential fit to a couple of traces registered one at the blue and one at the red edge of the emission spectrum was performed and the lifetimes were averaged. To perform

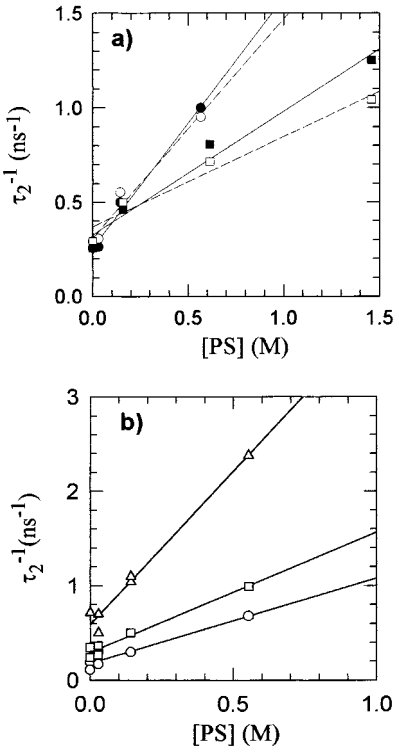

Figure 9. Stern−Volmer plots for the fastest component of the biexponential fit to the fluorescence emission decays (τ_2 in the text) monitored at 405 nm. Values of the linear fit parameters are given in Table 3. (a) At 27 °C in toluene mixtures with a polar solvent. Key: open circles, AMP in ethanol; filled circles, AP in ethanol; open squares, AMP in acetonitrile; filled squares, AP in acetonitrile. Full lines are the linear regressions of the data for AP (filled symbols), and dashed lines are the ones corresponding to AMP (open symbols). (b) In toluene−ethanol mixtures at 6 °C (circles), 27 °C (squares), and 61 °C (triangles).

the fit, the time dependences of excited-state concentrations were assumed to be

$$[\mathrm{AP}^*] = A_1 \exp(-t/\tau_1) + A_2 \exp(-t/\tau_2)$$

$$[\mathrm{AP{-}PS}^*] = B_1[\exp(-t/\tau_2) - \exp(-t/\tau_1)] \qquad (5)$$

The spectral distributions of the emission of AP* and of AP−PS* were assumed to be Gaussian. The parameters for the spectra were derived from the fits of $\nu_{max}(t)$: the values at $t \rightarrow 0$ were assigned to AP*, while those at $t \rightarrow \infty$ were assigned to AP−PS*.

The dependence of τ_2 with solvent composition is shown in Figure 9 for AMP and AP in tol−eth and tol−acn mixtures. They show Stern−Volmer type behavior as predicted by the mechanism, thus confirming that the spectral shift is caused by a dynamic process that is diffusion controlled.

The values of the ordinate and the intercept of these representations are summarized in Table 3 for different systems, together with the Arrhenius parameters of these rate constants for AP in tol−eth, [eth] = 0.145 M. The values of k_d (the slope of the Stern−Volmer plot according to eq 4) and its activation energy are consistent with what is expected for diffusion-limited rate constants in the media.[28]

The excited-state decay depicted by eq 3 is a two-state model. Aminophthalimides are considered a typical example of excited-state decay involving many states.[9,12,13,23] The decay in neat solvents can be described by an ensemble of excited states with different numbers of relaxed solvent molecules.[22] Solvent

SCHEME 1: Kinetic Mechanism for the Stepwise Solvent Exchange Model

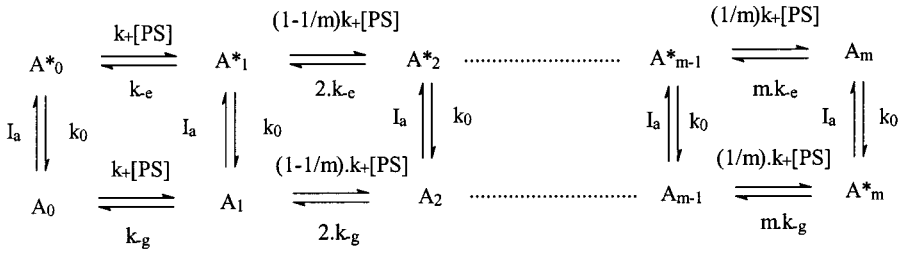

TABLE 3: Values of the Ordinate and Slope of the Stern−Volmer Representations Like Those of Figure 9 in Mixtures of a Polar Solvent with Toluene[a]

compd	polar solvent	*T* (°C)	ordinate (10^8 s^{-1})	slope (10^9 M^{-1} s^{-1})
AP	ethanol	6	1.77	0.90
AP	ethanol	27	2.6	1.32
AP	ethanol	61	5.9	3.2
AMP	ethanol	27	3.1	1.16
AP	acetonitrile	27	3.3	0.65
AMP	acetonitrile	27	3.7	0.48

compd	polar solvent	Arrhenius params	ordinate	slope
AP	ethanol	A	2.7×10^{11} s^{-1}	2.1×10^{12} M^{-1} s^{-1}
		E_a/kJ·mol^{-1}	17	18

[a] Arrhenius parameters for ordinate and slope of AP in toluene−ethanol.

molecules surrounding the solute are allowed to be in two states, corresponding to equilibrium with the solute before and after excitation. Each solvent molecule relaxation shifts the emission spectrum to the red by a fixed amount of energy. If *m* is the assumed fixed amount of solvent molecules in the solvation sphere, there are $m + 1$ different emitting states.

In solvent mixtures near room temperature, a behavior is observed similar to that in neat polar solvents at low temperature. In a model analogous to the one depicted in the previous paragraph, we postulate a stepwise relaxation by solvent exchange. We assume that the solvation sphere of a solute can accommodate *m* solvent molecules, independent of the composition of this solvation sphere. The solvation sphere can differ in composition from the bulk, and its state at constant *T* and *P* can be characterized by the number *n* of PS molecules (the number of nonpolar, NP, solvent molecules is then $m - n$).

A change of state involves either an incorporation of a PS molecule and a corresponding exit of an NP molecule or vice versa. From the kinetic point of view, the frequency of exit and entrance of a PS molecule depends on the occupation number, *n*, and on the bulk concentration of PS, and they are given by $k_-(n)$ and $k_+(n)$[PS], respectively, where *n* is the number of PS molecules previous to the exchange. If we make an analogy of this situation with a Langmuir type adsorption, then each PS molecule is an occupied adsorption site, and if we assume that these sites are independent, $k_-(n) = nk_-$ and $k_+(n) = (1 - n/m)k_+$.

Previous to excitation, the ground state is equilibrated with respect to solvation. For low concentrations of PS, the solvatochromic shift in the absorption of aminophthalimides is small. We can assume that the absorption coefficient is the same for all solute environments, and thus, the composition of the solvation sphere of excited molecules immediately after excitation coincides with the equilibrium distribution in the ground state.

In the excited state, PS molecules interact more strongly with the solute. From the kinetic point of view this means that the exit frequency of a PS molecule from the solvation sphere in the excited state (k_{-e}) is smaller than in the ground state, i.e., $k_{-e} < k_{-g}$. We assume that $k_+(n)$ is not affected by the existence of an excited state as this rate constant depends on diffusion in the bulk.

We further assume that the decay rate constant of the excited state (k_0) is independent of *n*. This assumption is justified by the fact that the fluorescence lifetime and quantum yield of the aminophthalimides remain almost constant in a variety of solvents, including polar and nonpolar ones.[16,18] This assumption may fail in HBD-rich environments.

The kinetic mechanism is summarized in Scheme 1. The solution of the differential equations is performed in the Appendix. In Scheme 1, A_n and A_n^* designate a ground state or an excited state, respectively, both with *n* PS molecules in the solvation sphere.

The kinetic equations of a similar mechanism were thoroughly worked out by Tachiya,[29] who used it to analyze the quenching of micelle-solubilized excited states. A similar kinetics was used by Moore et al. to describe excited-state decay in water−ethanol mixtures.[11] Langmuir association of solvent to solutes, as the present assumptions lead to, was also observed for ions in supercritical water,[30] a system with greater interaction energy than the ones treated in this work.

The conclusions of the mathematical treatment performed in the Appendix is given in what follows.

(i) The time-dependent concentration of A_n^* is given by eq 6 (which coincides with eq A13):

$$[A_n^*](t) = [A^*](0)\exp(-k_0 t)\binom{m}{n}(p_+(t))^n(p_-(t))^{(m-n)} \quad (6)$$

$$p_+(t) = p_{+e} + [p_{+g} - p_{+e}]\exp(-k_{ex}t) = 1 - p_-(t) \quad (7)$$

$$p_{+e,g} = k_+[PS]/(mk_{-e,g} + k_+[PS]) \quad (8)$$

$$k_{ex} = (mk_{-e} + k_+[PS])/m \quad (9)$$

The binomial-type distribution of PS around a solute is maintained throughout the decay. The decay of the total excited-state population, $[A^*](t) = \Sigma[A_n^*](t)$, is single exponential with a lifetime k_0.

(ii) The average number of PS molecules in the solvation sphere $\langle n\rangle(t) = mp_+(t)$ changes monoexponentially after excitation with a lifetime k_{ex}, according to eq 7.

(iii) We assume that the emission distribution of each A_n^* is Gaussian with equal width, σ, and with a maximum that shifts

TABLE 4: Kinetic and Spectral Data for AP in tol−eth, [eth] = 0.145 M[a]

T (°C)	k_+ (10^9 M^{-1} s^{-1})	k_{-g} (ns^{-1})	k_{-e} (ns^{-1})	k_0 (ns^{-1})
6	6.58	0.41	0.059	0.093
27	14.8	1.11	0.16	0.066
61	16.2	3.38	0.41	0.066

	E_a (kJ/mol)	log [A]		E_a (kJ/mol)	log [A]
k_+ (M^{-1} s^{-1})	12 ± 6	12 ± 1	k_{-e} (s^{-1})	28 ± 3	12.8 ± 0.5
k_{-g} (s^{-1})	30 ± 2	14.2 ± 0.3			

T (°C)	ν_{tol}^{abs} (10^3 cm^{-1})	ν_{tol}^{em} (10^3 cm^{-1})	ν_{eth}^{abs} (10^3 cm^{-1})	ν_{eth}^{em} (10^3 cm^{-1})	$[\Delta G_{0,tol} - \Delta G_{0,eth}]$ (kJ/mol)	$[\Delta G_{g(0,m)}{}^0 - \Delta G_{e(0,m)}{}^0]$ (kJ/mol)	m
6	28.5	23.3	26.7	18.9	37	15	4
						36	8
						43	9
27	28.6	23.6	26.9	19.1	37	19	4
						33	7
						38	8
61	28.8	23.9	27.1	19.3	38	22	4
						36	6
						41	7

[a] Errors are as follows: frequencies, ±100 cm^{-1}; ΔG, ±2 kJ/mol; rate constants, ±20%.

to the red, linearly with n, as depicted by eqs 10 and 11,

$$f_n(\nu) = \frac{1}{\sqrt{2\pi}\sigma} \exp\left(-\frac{(\nu - \nu_n)^2}{2\sigma^2}\right) \quad (10)$$

$$\nu_n = \nu_{NP} - n(\nu_{NP} - \nu_{PS})/m = \nu_{NP} - n\Delta\nu \quad (11)$$

where ν_{NP} and ν_{PS} are the emission maxima in the neat nonpolar and polar solvent components, respectively.

The decay at a fixed wavelength is given by

$$I(\nu,t) = \sum_n f_n(\nu) k_f [A_n^*](t) \quad (12)$$

in which we assume that k_f, the radiative rate constant, is independent of n. The decay is multiexponential with lifetimes in the arithmetic progression $k_0 + nk_{ex}$, $n = 0, ..., m$.

(iv) The mean emission wavenumber, $\langle\nu\rangle(t)$ changes as $\langle n\rangle(t)$, i.e., monoexponentially with a lifetime k_{ex}. As we can verify experimentally that spectra are symmetrical with respect to the maximum, $\langle\nu\rangle(t) = \nu_{max}(t)$.

There are five fitting parameters in the kinetic mechanism, k_+, k_{-g}, k_{-e}, k_0, and a total amplitude, which can be represented by [A*](0). They can be conveniently grouped in the set p_{-g}, p_{-e}, A_0^*, k_{ex}, and k_0. The value of m cannot be fitted, as the equations depend on it on a discrete manner. Instead m was systematically varied from 1 (a biexponential fit) to 9 to perform the different fits. A global analysis of the decays at various wavelengths was carried out to derive the fitting parameters summarized in Table 4. There is an appreciable improvement in the quality of the fit when m is increased from 1 to 4, accompanied by a significant change in the best-fit values of p_{-g}, p_{-e}, A_0^*, and k_{ex}. Increasing m from 4 to 9 improves only slightly the fit and changes the fitting parameters very little. On the contrary, k_0 is insensitive to the value of m. This fact is reasonable as k_0 is obtained from the long-time behavior of the decay, when the exchange is finished.

To completely determine the behavior of the system, the kinetic analysis can be integrated with spectroscopic data in a thermodynamic cycle of Gibbs free energy (see eq 15 below). The Gibbs free energy change for solvent exchange can be calculated from the kinetic rate constants k_+, k_{-g}, and k_{-e}, according to

$$K_{n-1,n}{}^g = \frac{[A_n]}{[A_{n-1}][PS]} = \frac{k_+\left(1 - \frac{n-1}{m}\right)}{nk_{-g}} = K_0{}^g\left(\frac{1}{n} - \frac{n-1}{n.m}\right) = \exp\left(-\frac{\Delta G_{g(n-1,n)}{}^0}{RT}\right) \quad (13)$$

$$K_{n-1,n}{}^e = \frac{[A_n^*]}{[A_{n-1}^*][PS]} = \frac{k_+\left(1 - \frac{n-1}{m}\right)}{nk_{-e}} = K_0{}^e\left(\frac{1}{n} - \frac{n-1}{nm}\right) = \exp\left(-\frac{\Delta G_{e(n-1,n)}{}^0}{RT}\right) \quad (14)$$

The Gibbs free energy variation for changing from a pure toluene to a pure ethanol solvation sphere of m solvent molecules can be calculated by adding all steps represented by eqs 13 and 14 from $n = 1$ to m for the ground state and for the excited state. These values are represented by $\Delta G^0{}_{g(0,m)}$, and by $\Delta G^0{}_{e(0,m)}$, respectively, in eq 15.

$$\Delta G_{0,tol} + \Delta G_{e(0,m)}{}^0 - \Delta G_{0,eth} - \Delta G_{g(0,m)}{}^0 = 0 \quad (15)$$

$\Delta G_{0,tol}$ and $\Delta G_{0,eth}$ are the Gibbs free energy differences between the relaxed excited state and the relaxed ground state of AP in pure toluene and in pure ethanol, respectively. They are approximated by[31]

$$\Delta G_{0,tol} = \frac{1}{2} N_A ch(\nu_{tol}{}^{abs} + \nu_{tol}{}^{em}) \quad (16)$$

$$\Delta G_{0,eth} = \frac{1}{2} N_A ch(\nu_{eth}{}^{abs} + \nu_{eth}{}^{em}) \quad (17)$$

where N_A is Avogadro's number, c is the speed of light, and h is Planck's constant.

The frequency values of the right members in eqs 16 and 17 are taken as the maxima of absorption and emission in neat toluene and ethanol. In this way, eq 15 can be used to verify the value of m used to derive the rate constants in a consistent iterative way. This was performed as follows: The fluorescence decay data were fitted beginning with a given value of m. The rate constants were used to calculate $\Delta G^0{}_{g(0,m)}$, and $\Delta G^0{}_{e(0,m)}$ and find the best value of m that verifies eq 15; this new estimate of m was used to repeat the cycle. This method was applied to the kinetic data in tol−eth, [eth] = 0.145 M. According to the results summarized in Table 4, the best value for m is 8 ± 1. A value of $m = 4$, though probably acceptable from the kinetic point of view, is evidently far from satisfying the thermodynamic conditions as shown in Table 4.

Discussion

Polarity as well as HBD capacity of the solvents are important in the solvation of AP and AMP. In the literature an increase in the dipole moment is obtained for AP excitation by semiempirical calculations.[7] The results of our calculations point additionally to an enhanced affinity of the excited state of the probes for HBD solvents, in agreement with other authors.[14] Even though hydrogen bond acceptor solvents (HBA; this capacity is quantified by the solvation parameter β[1,5]) interact with the ground and excited states of the probes, this interaction has very little contribution to the Stokes shift. This is demon-

strated by the very different Stokes shifts measured in triethylamine ($\Delta\nu = 5260$ cm^{-1}, $\beta = 0.71$), ethanol ($\Delta\nu = 7800$ cm^{-1}, $\beta = 0.75$), and trifluoroethanol ($\Delta\nu = 8860$ cm^{-1}, $\beta = 0$), as displayed in Figure 2.

As it was found for similar compounds,[26] coplanarity of the amino group with the aromatic ring and coupled ICT contribute appreciably to the Stokes shift of aminophthalimides. This fact explains the big $\Delta\nu$ in toluene, as well as the increase in dipole moment and hydrogen bond interaction upon excitation.

The behavior of the Stokes shift in solvent mixtures compared to neat solvents can be understood at the light of the solvation change in the excited state. As the fluorescence decay demonstrates, the probe environment changes during the excited-state lifetime. Therefore, a single solvation parameter is insufficient to characterize the solvation state of the probe. This is the reason steady-state Stokes shifts in mixtures differ from the values in neat solvents of the same bulk solvent parameters (for example $E_T(30)$). The departure increases with the difference in solvation between the components of the mixture, as the results in tol−eth and tol−acn depict in Figure 2. It is idle to discuss if aminophthalimides have the same solvent enrichment as the solvatochromic probes used to define solvent scales, because the solvation spheres of AP and AMP change with time.

The thermochromic behavior, as displayed in Figure 4, is linear due to the restricted temperature range in which the data were recorded. At much lower temperatures, solvent exchange will become much slower than excited-state decay, and thus, the exchange will not contribute to the spectral shift. The thermochromic effect will be solely due to solvent reorientation in the solvation sphere at fixed solvent composition, and the temperature variation of ν_{em} will decrease to values comparable to those in neat solvents. At very high temperatures, entropic factors dominate and the difference in composition between the bulk and the solvation sphere will tend to disappear. This effect will also decrease the temperature variation of ν_{em}. The contribution of solvent exchange to the thermochromism is, therefore, important in a temperature range where it is not much slower than excited-state decay and where equilibrium (entropic) factors do not compensate for the difference in interaction energy between the components of the mixture. This explains the maximum in the slopes of Figure 4 with composition. Factors as solvent composition, solvent viscosity, excited-state lifetime of the probe, and difference in interaction energy between the probe and the components of the mixture tune the temperature interval where the exchange effect is maximum.

The exchange kinetic mechanism adopted in this work to explain the time dependence of fluorescence is more complex than the biexponential description, which renders a description of quality comparable to that of the fluorescence decay. Nevertheless the exchange mechanism provides deeper insight into the solvation dynamics and is more rewarding, from the point of view of not only kinetics but also spectroscopic and thermodynamic aspects.

From the point of view of the calculations, the biexponential model has 5 fitting parameters (A_1, A_2, B_1, τ_1, τ_2 from eq 5), of which 2 are lifetimes and 3 are amplitudes of decays. Additionally it has spectroscopic parameters that are picked from the emission characteristics as $t \rightarrow 0$ and $t \rightarrow \infty$. This self-consistent choice is one of the reasons for its success in describing the data but limits the information it provides.

From the mechanistic point of view, a biexponential behavior can be explained by a two-state model, as described by eqs 3 and 4.[21] It is a simplification, as well as a first approach, to assume that only one PS molecule interacting with the excited state is responsible for the whole energy change of this state. Moreover, the fact that the emission spectrum obtained after relaxation is dependent on solvent composition is evidence that PS has an influence on the energy of the complex AP−PS. In other words, more than one PS molecule affects the excited-state energy. In this description a different emission spectrum is needed for AP* and (AP−PS)* at each solvent composition.

The exchange mechanism has also 5 adjustable parameters, of which 4 are rate constants, k_+, k_{-g}, k_{-e}, and k_0, and one is an amplitude, [A*](0). The total number of solvating molecules, m, has to be specified. The spectral characteristics are obtained from steady-state emission spectra in the neat components of the mixture, and a linear shift in energy is assumed for the spectra of intermediate solvation states. These spectra do not change with bulk solvent composition. Furthermore, m can be obtained in a self-consistent way that satisfies a thermodynamic cycle.

A two-state mechanism can be obtained as a particular case of the exchange mechanism for $m = 1$. This gives a very poor description of the kinetics if the spectral constraints are maintained, i.e., if the emission spectrum of AP* is the one in neat NP, and the emission spectrum of (AP−PS)* is the one in neat PS, and the decay amplitudes are linked by the condition that k_0 (eq 6) and k_f (eq 12) are constant. Because of the relaxation of these two conditions, the fit of eq 5 is much better than the fit to an exchange scheme with $m = 1$.

The two-state mechanism assumes that there is one preferred PS molecule that interacts very strongly with the excited state and that a number of other PS molecules stabilize the (AP−PS)* complex with an average continuum-like contribution. On the other hand, the exchange mechanism assumes that m PS molecules interact independently with the same energy with AP or AP*. This interaction takes place in an on−off way. A more realistic description of the interaction is surely that of a number of PS molecules interacting each in a different way with AP*, with a continuous variation of interaction energy depending on molecular distance. This can only be simulated by molecular dynamics and cannot be formalized easily in a kinetic mechanism. In view of this last picture, the mechanisms of eq 3 and Scheme 1 can be regarded as extreme cases, each one making different assumptions about the extent of interaction of the probe with each solvent molecule.

Additional experimental evidence sheds light on the success of the exchange mechanism. As shown in Figure 7, and summarized in Table 2, the spectral shift and the decay of the total emission are single exponential with rate constants that match those predicted by the exchange mechanism. The fact that $I_{max}(t)$ decays in a single exponential way can be explained if solvent exchange does not alter the emission probability of the total excited ensemble; i.e., solvent exchange only changes the energy of the emitted light but does neither quench nor enhance its probability. This is a support for the assumption that k_0 and k_f are constant. Furthermore, $\nu_{max}(t)$ also changes monoexponentially as predicted by eqs A18 and A14. This can only be obtained if the environment relaxation takes place with a single characteristic lifetime. In Scheme 1 this lifetime is the single step solvent exchange, represented by the rate constant k_{ex}.

Finally, the values obtained for the fitted parameters in the exchange mechanism are quite reasonable. The value of m is realistic for an aminophthalimide surrounded by ethanol or toluene molecules. The values of k_+ are those expected for diffusion-controlled rate constants in the solvent mixtures employed, and its activation energy is similar to the activation

energy of viscosity. An advantage of the exchange mechanism, which the other lacks, is that it allows one to determine the solvation of the ground and excited states of the aminophthalimides as a function of temperature and solvent composition.

Acknowledgment. C.C., R.F.-P., and P.F.A. are members of Carrera del Investigador Científico (Research Staff) from CONICET (Consejo Nacional de Investigaciones Científicas y Técnicas of Argentina). The work was supported by Grants TW10 and TX28 from Universidad de Buenos Aires, PID 0388 (CONICET), PICT 4438 and 0647 (ANPCyT, Argentina), and A-13622/1-12 from Fundación Antorchas (Argentina). We acknowledge Dr. Darío Estrín (INQUIMAE, Universidad de Buenos Aires) for DFT calculations and valuable discussion.

Appendix

The differential equations that follow from Scheme 1 after a $\delta(t)$ pulse excitation are given by eqs A1:

$$\frac{d[A_0^*]}{dt} = k_{-e}[A_1^*] - (k_+[PS] + k_0)[A_0^*]$$

$$\frac{d[A_n^*]}{dt} = \left(1 - \frac{n-1}{m}\right)k_+[PS][A_{n-1}^*] + (n+1)k_{-e}[A_{n+1}^*] - \left(\left(1 - \frac{n}{m}\right)k_+[PS] + nk_{-e} + k_0\right)[A_n^*] \quad n = 1, \ldots, m-1$$

$$\frac{d[A_m^*]}{dt} = \frac{1}{m}k_+[PS][A_{m-1}^*] - (mk_{-e} + k_0)[A_m^*] \quad \text{(A1)}$$

At equilibrium, the mean occupation number ($\langle n \rangle$) has a Langmuir-type dependence on [PS] as given by eq A2 for the ground state:

$$\langle n \rangle_g = m\frac{k_+[PS]}{mk_{-g} + k_+[PS]} \quad \text{(A2)}$$

Correspondingly, the probability of finding a solute with an occupation number n, P_n, has a binomial distribution at equilibrium, as given by

$$(P_n)_{e,g} = \frac{m!}{n!(m-n)!}(p_{+e,g})^n(p_{-e,g})^{(m-n)}$$

$$p_{+e,g} = \frac{\langle n \rangle_{e,g}}{m} = \frac{k_+[PS]}{mk_{-e,g} + k_+[PS]} = 1 - p_{-e,g} \quad \text{(A3)}$$

where p_+ and p_- are the probabilities of finding a PS or an NP molecule in the solvation sphere, respectively, and subindexes e and g refer to the excited state and to the ground state, respectively. All four variables, $\langle n \rangle$, P_n, p_+, and p_- have a value for the ground state different from that for the excited state.

The model depicted here is a particular case of the work of Tachiya.[19] On one side, there is no quenching of the excited state by PS, and this can be easily taken into account by setting the quenching rate constant equal to zero. On the other hand, the equations must be modified to take into account the different value for the exit rate constant in the excited and ground states of the solute.

The $m + 1$ differential equations of eqs A1 were solved by Tachiya using a generating function $F(s,t)$, defined by

$$F(s,t) = \sum_{n=0}^{m} s^n[A_n^*](t) \quad \text{(A4)}$$

where s is an arbitrary parameter, so that $F(1,t)$ equals the time-dependent total excited-state concentration and $[A_n^*](t)$ can be derived from $F(s,t)$ by eq A5:

$$[A_n^*](t) = \frac{1}{n!}\left(\frac{\partial^n F(s,t)}{\partial s^n}\right)_{s=0} \quad P_n(t) = \frac{[A_n^*](t)}{\Sigma[A_n^*](t)} = \frac{[A_n^*](t)}{[A^*](t)} \quad \text{(A5)}$$

To simplify the notation, we define

$$a_g = mk_{-g} \quad a = mk_{-e} \quad b = k_+[PS] \quad \text{(A6)}$$

so that the probabilities at equilibrium can be written $p_{+g} = a_g/(a_g + b)$, $p_{+e} = a/(a + b)$, and $p_{-e,g} = 1 - p_{+e,g}$.

The generating function has the general solution

$$F(s,t) = (s-1)^{-m.k_0/a+b}\left(s + \frac{a}{b}\right)^{(m+m.k_0/a+b)}[G(y)] \quad \text{(A7)}$$

$$y(s,t) = \left(\frac{s-1}{s + a/b}\right)\exp\left(-\frac{a+b}{m}t\right) \quad \text{(A8)}$$

The function $G(y)$ is determined by the initial condition. In this case, we assume that the population immediately after excitation coincides with the ground-state population. Introducing eq A3 into eq A4 gives

$$F(s,0) = [A^*](0)\left(\frac{a_g + bs}{a_g + b}\right)^m = (s-1)^{-m.k_0/a+b}\left(s + \frac{a}{b}\right)^{(m+m.k_0/a+b)}\{G[y(s,0)]\} \quad \text{(A9)}$$

Replacing $G(y)$ into eq A7 gives

$$F(s,t) = [A^*](0)\, e^{-k_0 t}\left[\frac{a+bs}{a+b} - \frac{b(a_g - a)(s-1)}{(a_g + b)(a+b)}\exp\left(-\frac{(a+b)}{m}t\right)\right] \quad \text{(A10)}$$

which can be rearranged in the form

$$F(s,t) = [A^*](0)\, e^{-k_0 t}[p_-(t) + p_+(t)s]^m \quad \text{(A11)}$$

In eq A11 it is evident that the total excited-state population, $[A^*](t) = [A^*](0)\exp[-(k_0 t)]$, decays such as a single exponential, with a rate constant k_0. In eq A11, $p_+(t)$ and $p_-(t)$ are

the time-dependent occupation probabilities, which change from the ground-state values $p_{+,-g}$ at $t = 0$ to the excited-state values $p_{+,-e}$ at $t \rightarrow \infty$ in an exponential way:

$$p_+(t) = p_{+e} + [p_{+g} - p_{+e}] \exp\left(-\frac{a+b}{m}t\right) \quad \text{(A12)}$$

The relaxation time from eq A12, $k_{ex} = (mk_{-e} + k_+[PS])/m$, can be interpreted as the exchange relaxation time/solvation site.

Equation A5 can now be used to obtain the time-dependent population, which has the form

$$[A_n^*](t) = [A^*](t)\binom{m}{n}(p_+(t))^n(p_-(t))^{(m-n)} \quad \text{(A13)}$$

The probability $P_n(t)$ remains binomial along the whole relaxation. The decay of each A_n^* is multiexponential, with $m + 1$ terms with lifetimes in the arithmetic progression $k_0 + nk_{ex}$, $n = 0, ..., m$.

The mean occupation number of the solvation sphere is $\langle n\rangle(t)$, which is given by

$$\langle n\rangle(t) = \frac{(\partial F(s,t)/\partial s)_{s=1}}{[A^*](t)} = mp_+(t) = \langle n\rangle_e + (\langle n\rangle_g - \langle n\rangle_e)\exp(-k_{ex}t) \quad \text{(A14)}$$

Equation A14 shows that $\langle n\rangle(t)$ changes in an exponential way determined by the exchange relaxation rate constant, k_{ex}.

To obtain the time-resolved emission spectra, we have to make some assumptions on the individual fluorescence spectrum of each environment of A_n^*; i.e., we have to assign a fluorescence spectrum, $f_n(\nu)$, to each A_n^*. We assume that $f_n(\nu)$ are all Gaussian functions with the same bandwidth (σ) and with a shift to the red that is linear with n, $\Delta\nu$ being the shift caused by each PS molecule.

$$f_n(\nu) = \frac{1}{\sqrt{2\pi}\sigma}\exp\left(-\frac{(\nu - \nu_n)^2}{2\sigma^2}\right) \quad \text{(A15)}$$

$$\nu_n = \nu_{NP} - n(\nu_{NP} - \nu_{PS})/m = \nu_{NP} - n\Delta\nu \quad \text{(A16)}$$

In eq A16 ν_{NP} and ν_{PS} are the maxima of the emission spectra in the pure solvents.

The time-dependent spectra are obtained from

$$I(\nu,t) = \sum_n f_n(\nu)k_f[A_n^*](t) \quad \text{(A17)}$$

where k_f is the emission rate constant, which is assumed to be independent of n. Equation A17 indicates that the decay at fixed wavelength is a multiexponential with the same lifetimes as $A_n^*(t)$.

The mean frequency of the emission spectrum is

$$\langle\nu\rangle(t) = \frac{\int_{-\infty}^{\infty}\nu I(\nu,t)\,d\nu}{\int_{-\infty}^{\infty}I(\nu,t)\,d\nu} = \nu_{NP} - \langle n\rangle(t)\Delta\nu \quad \text{(A18)}$$

The last equation is obtained by replacing $I(\nu,t)$ from eq A17 and taking into account eq A16 and the fact that $f_n(\nu)$ from eq A15 is normalized. From eq A18 we can deduce that $\langle\nu\rangle(t)$ also relaxes in a single-exponential way with the rate constant k_{ex}.

References and Notes

(1) Reichardt, C. *Chem. Rev.* **1994**, *94*, 2319.
(2) Lakowicz, J. R. *Principles of Fluorescence Spectroscopy*, 2nd ed.; Kluwer Academic, Plenum Publishers: New York, 1999; Chapter 6.
(3) Matyushov, D. M.; Voth, G. A. *J. Chem. Phys.* **1999**, *111*, 3630.
(4) Khajehpour, M.; Kauffman, J. F. *J. Phys. Chem. A* **2000**, *104*, 9512.
(5) Marcus, Y. *Chem. Soc. Rev.* **1993**, *22*, 409.
(6) Bosch, E.; Rosés, M. *J. Chem. Soc., Faraday Trans.* **1992**, *88*, 3541.
(7) Suppan, P. *J. Chem. Soc., Faraday. Trans. 1* **1987**, *83*, 495.
(8) Suppan, P. *J. Photochem. Photobiol., A* **1990**, *50*, 293.
(9) Mazurenko, Y. T.; Bakshiev, N. K. *Opt. Spectrosc*. **1970**, *28*, 490.
(10) Chapman, C. F.; Fee, R. S.; Maroncelli, M. *J. Phys. Chem.* **1995**, *99*, 4811.
(11) Moore, R. A.; Lee, J.; Robinson, G. W. *J. Phys. Chem.* **1985**, *89*, 3648.
(12) Bakhshiev, N. G.; Mazurenko, Y. T.; Piterskaya, I. V. *Opt. Spectrosc*. **1966**, *21*, 307.
(13) Ware, W. R.; Lee, S. K.; Brant, G. J.; Chow, P. P. *J. Chem. Phys.* **1971**, *54*, 4729.
(14) Harju, T.; Huizer, A. H.; Varma, C. A. G. O. *Chem. Phys.* **1995**, *200*, 214.
(15) Laitinen, E.; Salonen, K.; Harju, T. *J. Chem. Phys.* **1996**, *105*, 9771.
(16) Soujanya, T.; Krishna, T. S. R.; Samanta, A. *J. Phys. Chem.* **1992**, *96*, 8544.
(17) Saroja, G.; Samanta, A. *Chem. Phys. Lett.* **1995**, *246*, 506.
(18) Das, S.; Datta, A.; Bhattacharyya, K. *J. Phys. Chem. A* **1997**, *101*, 3299.
(19) Datta, A.; Das, S., Mandal, D.; Pal, K.; Bhattacharyya, K. *Langmuir* **1997**, *13*, 6922.
(20) Yuan, D.; Brown, R. G. *J. Phys. Chem. A* **1997**, *101*, 3461.
(21) Betts, T. A.; Bright, F. V. *Appl. Spectrosc.* **1990**, *44*, 1203.
(22) Rapp, W.; Klingenberg, H. H.; Lessing, H. E. *Ber. Bunsen-Ges. Phys. Chem.* **1971**, *75*, 883.
(23) Lakowicz, J. R. *Principles of Fluorescence Spectroscopy*, 2nd ed.; Kluwer Academic, Plenum Publishers: New York, 1999; Chapter 7.
(24) Marcus, Y. *Ion Solvation*; John Willey and Sons Ltd.: Chichester, Great Britain, 1985; Chapter 6.
(25) Cortés, J.; Heitele, H.; Jortner, J. *J. Phys. Chem.* **1994**, *98*, 2527.
(26) Il'ichev, Y. V.; Kühnle, W.; Zachariasse, K. A. *J. Phys. Chem.* **1998**, *102*, 5670.
(27) Calculations performed by Dr. Dario Estrin (INQUIMAE, Universidad de Buenos Aires) with DFT predict an interaction energy of −26 kJ/mol between one ethanol molecule and AMP.
(28) Turro, N. J. *Modern Molecular Photochemistry*; Univ Science Books: Sausalito, CA, 1991; Chapter 9.
(29) Tachiya, M. *Chem. Phys. Lett.* **1975**, *33*, 289. Tachiya, M. *J. Chem. Phys.* **1982**, *76*, 340.
(30) Flanagin, L. W.; Balbuena, P. B.; Johnston, K. P.; Rossky, P. J. *J. Phys. Chem. B.* **1997**, *101*, 7998.
(31) Vath, P.; Zimmt, M. B.; Matyushov, D. V.; Voth, G. A. *J. Phys. Chem. B* **1999**, *103*, 9130.
(32) Soujanya, T.; Fessenden, R. W.; Samanta, A. *J. Phys. Chem.* **1996**, *100*, 3507.